

RESEARCH LETTER

10.1002/2014GL059229

Key Points:

- The settling depth in granular media is independent of gravity
- The settling time scales like $g^{-1/2}$
- Layering driven by granular sedimentation should be similar

Supporting Information:

- Readme
- Text S1

Correspondence to:

E. Altshuler,
ealtshuler@fisica.uh.cu

Citation:

Altshuler, E., H. Torres, A. González-Pita, G. Sánchez-Colina, C. Pérez-Penichet, S. Waitukaitis, and R. C. Hidalgo (2014), Settling into dry granular media in different gravities, *Geophys. Res. Lett.*, 41, 3032–3037, doi:10.1002/2014GL059229.

Received 7 JAN 2014

Accepted 10 APR 2014

Accepted article online 14 APR 2014

Published online 1 MAY 2014

Settling into dry granular media in different gravities

E. Altshuler¹, H. Torres¹, A. González-Pita¹, G. Sánchez-Colina¹, C. Pérez-Penichet¹, S. Waitukaitis², and R. C. Hidalgo³

¹“Henri Poincaré” Group of Complex Systems, Physics Faculty, University of Havana, Havana, Cuba, ²Department of Physics, James Franck Institute, University of Chicago, Chicago, Illinois, USA, ³Department of Physics and Applied Mathematics, University of Navarra, Pamplona, Spain

Abstract While the penetration of objects into granular media is well-studied, there is little understanding of how objects settle in gravities, g_{eff} different from that of Earth—a scenario potentially relevant to the geomorphology of planets and asteroids and also to their exploration using man-made devices. By conducting experiments in an accelerating frame, we explore g_{eff} ranging from 0.4 g to 1.2 g. Surprisingly, we find that the rest depth is independent of g_{eff} and also that the time required for the object to come to rest scales like $g_{\text{eff}}^{-1/2}$. With discrete element modeling simulations, we reproduce the experimental results and extend the range of g_{eff} to objects as small as asteroids and as large as Jupiter. Our results shed light on the initial stage of sedimentation into dry granular media across a range of celestial bodies and also have implications for the design of man-made, extraterrestrial vehicles and structures.

A loosely packed bed of sand sits precariously on the fence between mechanically stable and flowing states. This has especially strong implications not only for the geomorphology of the Earth but for that of extraterrestrial bodies where the surface is predominantly granular [Shinbrot et al., 2004; Almeida et al., 2008; Thomas and Robinson, 2005; Asphaug, 2007; Miyamoto et al., 2007]. Beyond surface morphology, extraterrestrial exploration and development requires navigation in and on loose granular media, but little is known regarding how objects settle in granular systems with gravitational conditions different from Earth’s. Such understanding may have helped prevent the difficulties encountered by the Mars rover, Spirit, as it sank into and tried to escape from a sand dune in 2009 (see, for example, <http://marsrover.nasa.gov/spotlight/20091019a.html>). Other endeavors, such as asteroid or lunar mining [Elvis, 2012], will certainly involve both navigation and construction on granular surfaces.

During the last decade, our understanding of the resistance to objects penetrating into granular media under Earth-like conditions has advanced quickly [Uehara et al., 2003; Walsh et al., 2003; Boudet et al., 2006; de Vet and de Bruyn, 2007; Katsuragi and Durian, 2007; Pacheco-Vázquez et al., 2011; Katsuragi, 2012; Kondic et al., 2012; Ruiz-Suárez, 2013]. A handful of attempts have mimicked low-gravity conditions [Goldman and Umbanhowar, 2008; Brzinski and Durian, 2010; Chen et al., 2009; Constantino et al., 2011; Dorbolo et al., 2013; Brzinski et al., 2013], mainly by using air-fluidized granular beds or grains immersed in a liquid, but the main focus has typically been on the role of intruder velocity or grain friction. Here we focus exclusively on the role of gravity as an object settles into granular media. By conducting experiments in a freely falling reference frame, we are able to create true low- and high-gravity conditions as a sphere gently settles into a loose granular bed. We confirm the previously reported [Goldman and Umbanhowar, 2008], but hereto unexplained, observation that the rest time, t_{rest} (i.e., the total time required for the object to come to rest), scales like $g_{\text{eff}}^{-1/2}$. We also find, surprisingly, that the rest depth, z_{rest} , is independent of g_{eff} . We confirm these results and extend the range of g_{eff} with the aid of discrete element modeling (DEM) simulations, which highlight the sudden transition from fluid-like to solid-like response when the sphere comes to rest. Finally, with a simple analytical model we show that the depth-dependent stopping force against penetration of an intruder into granular matter is proportional to the effective gravity, an hypothesis widely used, but never before verified in an experiment where the effective gravity is changed.

We vary g_{eff} using a five-story (15 m) tall Atwood machine in which one of the counterweights is a wireless “lab-in-a-bucket” (Figure 1). The cylindrical bucket (30 cm diameter by 26 cm depth) is filled with expanded polystyrene beads (average diameter $d = 5.0$ mm, density $\rho = 0.014 \pm 0.002$ g/cm³, and packing fraction $\phi = 0.68 \pm 0.01$). We choose this as our granular material because its low density facilitates the penetration

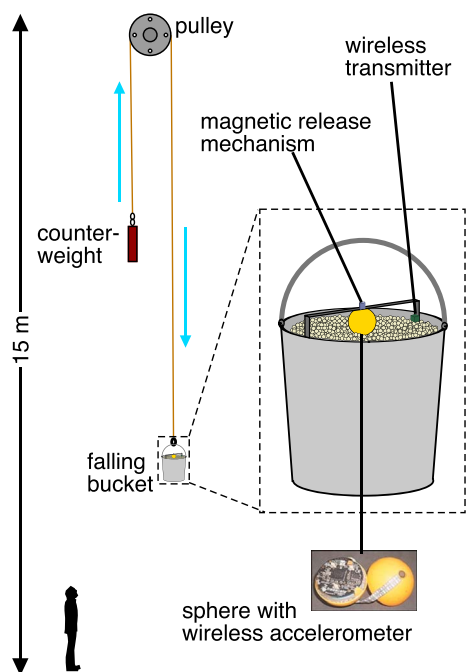


Figure 1. Freely falling granular laboratory. A five-story (15 m) tall Atwood machine controls the downward/upward acceleration of a 30 cm diameter laboratory in a bucket filled with the granular medium. As the bucket falls/rises, a sphere is released from rest and allowed to sink while “feeling” the effective gravity g_{eff} of the accelerating frame. We use an accelerometer embedded in the sphere for real-time measurement of the post-release acceleration.

magnetic trigger and occurring in the first ~ 50 ms), (ii) a second region of negative slope corresponding to the majority of the penetration process, and (iii) a third region of positive slope corresponding to sudden stopping of the sphere (a feature also seen in experiments performed at $g_{\text{eff}} = g$). We note the presence of a brief, damped oscillation that occurs near the instant the sphere comes to rest, which may signify the presence of a granular shock. The oscillations in the a versus t curves are not an experimental artifact but instead are real fluctuations from the granular medium (the simulations show similar oscillations). The minor differences between the curves in Figure 2 (especially those in region (i)) arise from the sensitivity to vibrations of the magnetic release system. Error bars are estimated from repeated runs of the same experiment (i.e., the same g_{eff}) and subsequent calculation of the standard deviation from the mean for the three representative parameters: the duration of the penetration process, the maximum (positive) acceleration, and the minimum (negative) acceleration (5 ms, 0.6 m/s², and 1.0 m/s², respectively). These relatively small errors are consistent with the fact that the “global” experimental features described below are reproducible not only for the set of curves displayed in Figure 2 but also for several other runs not included in the graph to avoid overcrowding. As we shall show shortly, the validity of these experimental results is also confirmed by discrete computer simulations.

Comparison of the different curves in Figure 2a shows that as g_{eff} decreases from approximately Uranus’ gravity to Mars’ gravity, the peak acceleration increases while the depth of the minimum decreases. Additionally, the duration of the process as a whole increases. This point is made particularly clear in Figure 2b, where we integrate a versus t and plot the velocity v versus t , which also shows that the maximum speed of the sphere increases with higher g_{eff} . In Figure 2c, we integrate once more to plot the distance traveled below the surface z versus t , which reveals the key observation that the rest depth z_{rest} is essentially the same for all g_{eff} (average value $z_{\text{rest}} = 14.0 \pm 0.6$ cm). If instead of plotting the a versus t we plot it against z (normalized by g_{eff} , as in Figure 2d), we collapse the data to a line with slight upward curvature (apart from the brief initial and final moments, corresponding to sections (i) and (iii), respectively).

of the intruder, thus making the experiments possible. Although it is lighter and indeed much softer than terrestrial or extraterrestrial soils, our results can be explained without any consideration of bead compression, which suggests that it behaves similarly to more “typical” granular media. Depending on the relative masses of the counterweight and bucket (plus contents), the laboratory can either fall or rise. As it does so, the bucket and the equipment inside it “feel,” for a few seconds, a gravitational acceleration, g_{eff} , different than g (smaller if it is falling and larger if it is rising). During the fall (or rise), we release a sphere (diameter $D = 4$ cm, mass $m = 23$ g) held at rest just above the free surface and let it sink into the granular medium. The sphere houses a three-axis wireless accelerometer in its interior, allowing us to record its instantaneous acceleration. The sphere/accelerometer is light enough to prevent the “infinite penetration” encountered by Pacheco-Vázquez *et al.* [2011] (For further experimental details, see supporting information.).

Figure 2a shows the sphere’s acceleration a versus time t relative to the Lagrangian frame of the moving bucket (normalized by $g = 9.8$ m/s²) for six values of g_{eff} (note that z positive points downward and that the data represent the proper acceleration of the sphere, i.e., the acceleration caused by the forces exerted on it by the granular medium). Each curve has three well-defined sections: (i) a region of positive slope associated with the release (caused by mag-

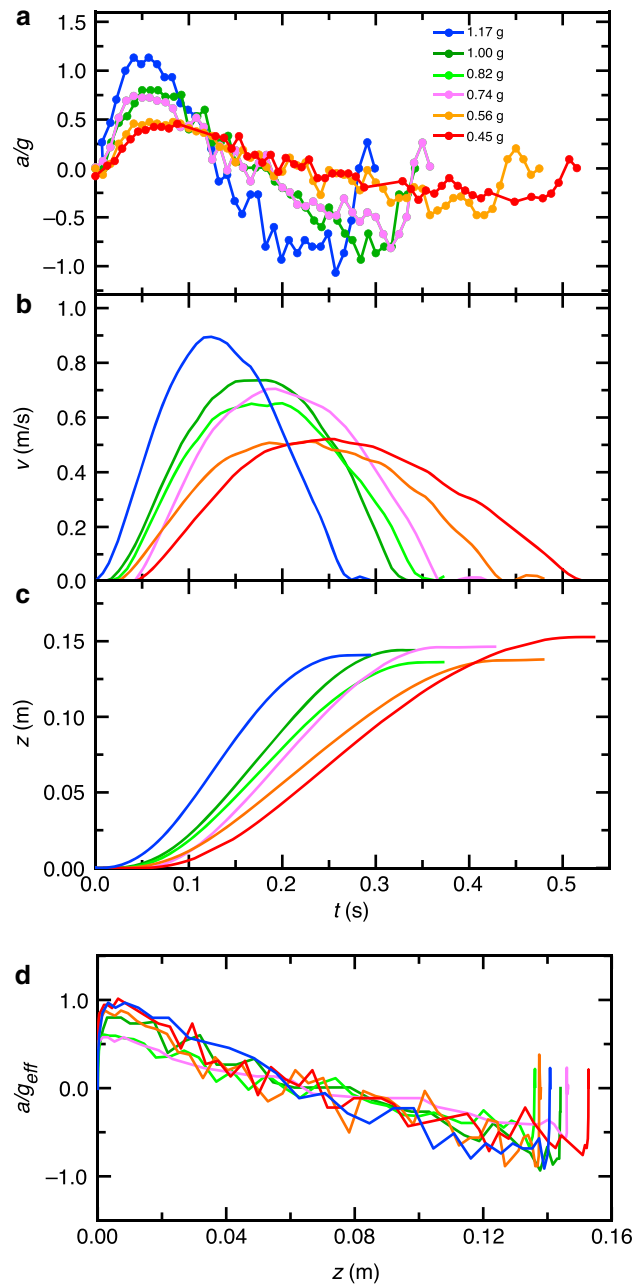


Figure 2. Experimental sink dynamics. (a) Sphere acceleration a/g versus time t for six representative values of g_{eff} . Values for g_{eff} are indicated in the legend in the figure and also correspond to following panels. (b) Time dependence of the sphere's velocity v via numerical integration of Figure 2a. (c) Time dependence of sphere's penetration z , calculated via integration of Figure 2b. (d) Normalized sphere acceleration a/g_{eff} versus penetration distance z .

Thus, the equation of motion can be approximated as

$$ma = mg_{eff} - \kappa \lambda (1 - e^{-(z/\lambda)}) \quad (2)$$

This quickly explains the shape of the a/g_{eff} versus z curves shown in Figure 2d (in particular reproducing the upward curvature). Fitting each of the a/g_{eff} versus z curves with equation (2) while using the bucket

Figures 3a–3d show the simulation results for similar gravitational accelerations to those used in the experiments. (For simulation details, see supporting information.) Several experimental features are reproduced quantitatively with no free parameters, e.g., the duration of the process, the size of the acceleration peaks, the maximum velocities, and the rest depth. Closer inspection reveals that the fluctuations in the acceleration become stronger as the sphere comes closer to stopping, likely indicative of the building up and breaking down of force chains (this will be the subject of future work). This suggests that the stopping and eventual static support of the intruder is associated with the medium transitioning from a fluidized to jammed state [Kondic *et al.*, 2012; Bi *et al.*, 2011].

In Figure 4, we plot the rest depth, z_{rest} (Figure 4a) and rest time, t_{rest} (Figure 4b) versus g_{eff} , which shows that z_{rest} is essentially independent of g_{eff} while t_{rest} scales like $g_{eff}^{-1/2}$. We can explain the scaling of the rest time with g_{eff} based on the work of Pacheco-Vázquez *et al.* [2011], who proposed a simple equation of motion for an object penetrating into a granular medium

$$ma = mg - \eta v^2 - \kappa \lambda (1 - e^{-(z/\lambda)}), \quad (1)$$

where m is the impactor mass, η characterizes inertial drag, κ is a friction-like coefficient related to the pressure in the granular medium (unit N/m), and λ is a characteristic length on the order of the width of the container. (The exponential term arises from the well-known Janssen effect in which the pressure in a granular system saturates at a finite depth owing to redistribution of weight to the container walls [Sperl, 2006].) For sufficiently large m , the combination of the inertial term ($\propto v^2$) and the saturating, depth-dependent term (i.e., the exponential) leads to “infinite penetration” of the projectile at a constant, terminal

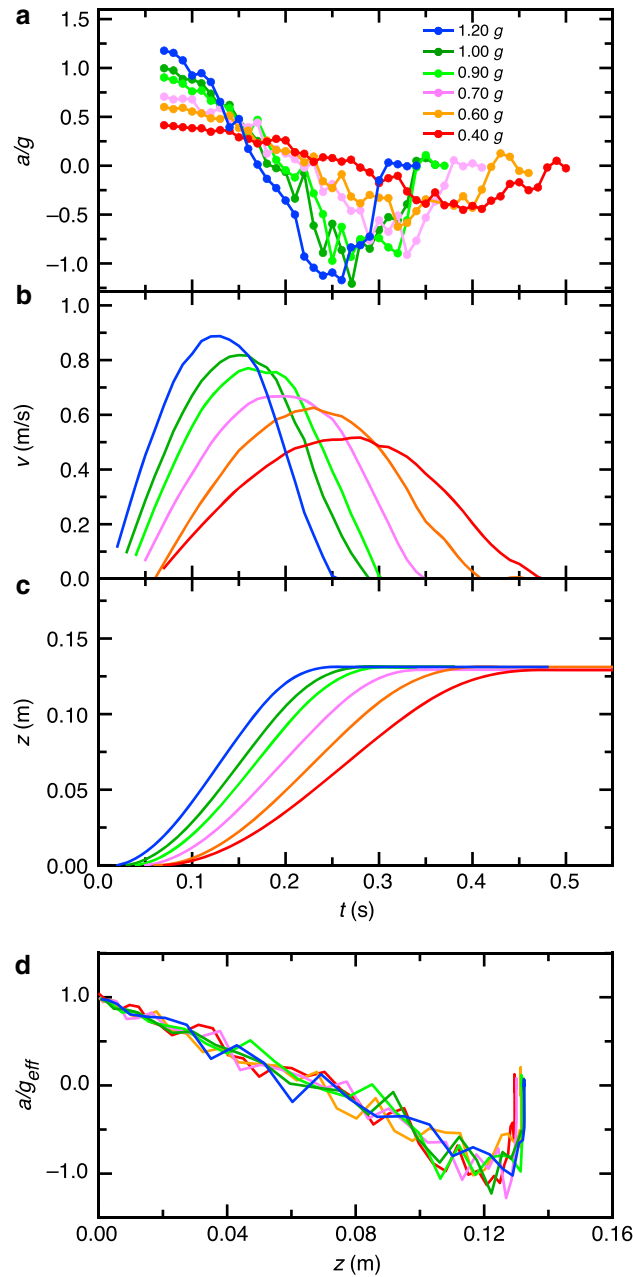


Figure 3. Simulation sink dynamics. (a) Sphere acceleration a/g versus time t for six representative values of g_{eff} . Values for g_{eff} are indicated in the legend in the figure and also correspond to the following panels. (b) Time dependence of the sphere's velocity v via numerical integration of Figure 4a. (c) Time dependence of sphere's penetration below free granular surface z , calculated via integration of Figure 4b. (d) Normalized sphere acceleration a/g_{eff} versus penetration distance z .

The term in the integral is independent of g_{eff} (as λ , α , and m are strictly independent of g_{eff} and z_{rest} is empirically so). This reveals that $t_{\text{rest}} \propto (l_c/g_{\text{eff}})^{1/2}$, where l_c is a characteristic length. In the limit $\lambda \rightarrow \infty$, it is easy to show that $l_c \propto z_{\text{rest}}$, and consequently, the whole problem can be rescaled in terms of t_{rest} and z_{rest} . For finite λ , the average stopping force is smaller and the ball penetrates further into the medium than this simple scaling would suggest. Nonetheless, in realistic geophysical situations where no confining walls are present, λ is indeed large and the simple scaling might prove very useful.

radius for the parameter λ and leaving κ as a free parameter, we find $\kappa = \alpha g_{\text{eff}}$, where $\alpha = 0.415 \pm 0.004 \text{ N s}^2/\text{m}^2$, as shown in Figure 4c. The proportionality between κ and α has been proposed before [Katsuragi and Durian, 2007; Constantino et al., 2011], but here we demonstrate its validity at gravities above and below g for the first time (and indeed even with a much lighter granular material). Taking into account the numerical value obtained for α , we point out that this depth-dependent term is *not* caused by “hydrostatic pressure.” If this were the case, we would expect $\alpha \approx \rho \pi D^2/4$. However, we find $\alpha/(\rho \pi D^2/4) \approx 34.6$, indicating that hydrostatic pressure adds just a small contribution to the depth-dependent force (in other experimental configurations, the equivalent ratio is smaller [Constantino et al., 2011]).

We can reconcile our phenomenological model with the observation that the rest time scales like $g_{\text{eff}}^{-1/2}$. To show this, we begin by rewriting equation (2) as

$$v \frac{dv}{dz} = g_{\text{eff}} \left[1 - \frac{\alpha \lambda}{m} (1 - e^{-z/\lambda}) \right]. \quad (3)$$

We integrate this equation with respect to z (with the initial conditions $z_0 = 0$ and $v_0 = 0$) to find

$$\frac{1}{2} v^2 = g_{\text{eff}} \left[z \left(1 - \frac{\alpha \lambda}{m} \right) - \frac{\alpha \lambda^2}{m} (e^{-z/\lambda} - 1) \right]. \quad (4)$$

Next, we isolate the velocity term, take the square root of both sides (note we are interested in $t_{\text{rest}} > 0$ and thus use the positive root), and integrate once more, which gives

$$t_{\text{rest}} = (2g_{\text{eff}})^{-1/2} \int_0^{z_{\text{rest}}} \left[z \left(1 - \frac{\alpha \lambda}{m} \right) + \frac{\alpha \lambda^2}{m} (1 - e^{-z/\lambda}) \right]^{-1/2} dz. \quad (5)$$

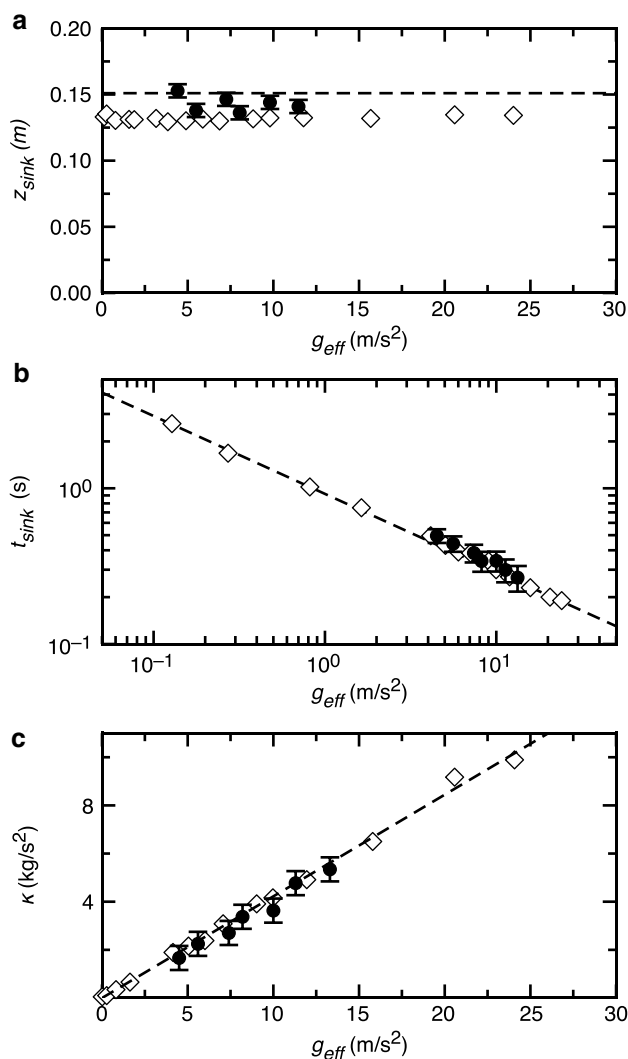


Figure 4. Penetration scalings. (a) Rest depth z_{rest} versus g_{eff} for experiment (black circles) and simulations (open diamonds). Dashed line is the predicted rest depth based on equation (6). (b) Rest time t_{rest} versus g_{eff} . Fit to simulation data is power law with exponent $-1/2$, as predicted in equation (5). (c) Frictional sink parameter κ versus g_{eff} . Values for κ are calculated from individually fitting a versus z curves to equation (3) with $\lambda = 15$ cm (i.e., the radius of the container holding the granular material). Symbols in Figures 4b and 4c are the same as in Figure 4a.

we make a counterintuitive observation that may have important implications for extraterrestrial navigation and engineering, namely that the rest depth of an object set on the surface of granular media is independent of the ambient gravitational acceleration. We explain this peculiar observation with a force law that includes a depth-dependent frictional term proportional to g_{eff} , which effectively removes any gravitational term from the equation of motion at the point of static equilibrium. From the point of view of surface morphology, our results suggest that the initial stage of sedimentation into granular media on different celestial bodies should be largely independent of local gravitational acceleration, i.e., the size of the body. Furthermore, this has the fortuitous implication that Earth-based experiments aimed at reproducing the conditions of robot navigation on permanent construction on another planet or asteroid should be performed without “adjusting” the mass for the extraterrestrial gravity conditions.

Finally, this model also leads to the conclusion that z_{rest} is independent of g_{eff} . When the sphere reaches its resting spot, the velocity vanishes, and thus, we can set the left-hand side of equation (4) to zero, i.e.,

$$\left(1 - \frac{\alpha\lambda}{m}\right)z_{\text{rest}} = \frac{\alpha\lambda^2}{m}\left(e^{-z_{\text{rest}}/\lambda} - 1\right). \quad (6)$$

This is a transcendental equation that cannot be solved analytically. However, quick inspection reveals that z_{rest} is independent of the gravitational acceleration as g_{eff} is not present. Moreover, we can use the experimental parameters $\lambda = 0.15$ m and $\alpha = 0.415$ Ns^2/m^2 to solve equation (6) numerically, which gives $z_{\text{rest}} \approx 0.15$ m, close to what we actually measure (0.14 ± 0.06 m). The fact that it is somewhat larger may result from ignoring the velocity term in equation (1), which would tend to make the sphere stop a little earlier. (Indeed, numerically solving equation (1) directly with the value for η from Pacheco-Vázquez et al. [2011] gives $z_{\text{rest}} = 0.14$ m, in better agreement still with the data from the experiments and simulations.)

To our knowledge, this work is the first to report on the full settling dynamics of an object into granular media at different gravities from that of Earth. By using a freely falling laboratory, we are able to investigate g_{eff} ranging roughly from the conditions of Mars to Uranus. We reproduce and extend this range with the aid of DEM simulations, which highlight the importance of transient force fluctuations in the penetration process that may be related to the continual buildup and breakdown of granular force chains. In both the experiments and simulations,

Acknowledgments

The data for this paper are available by contacting E. Altshuler (ealtshuler@fisica.uh.cu). The Spanish MINECO project FIS2011-26675, the PIUNA program (U. Navarra), and the Project 29942WL (Fonds de Solidarité Prioritaire France-Cuba) have partially supported this research. We acknowledge the collaboration of O. Ramos, J. Wu, A. J. Batista Leyva, and the Zeolites Group (IMRE, University of Havana). E. Altshuler thanks the late M. Álvarez-Ponte for inspiration.

The Editor thanks two anonymous reviewers for their assistance in evaluating this paper.

References

- Almeida, M. P., E. J. Parteli, J. S. Andrade Jr., and H. J. Herrmann (2008), Giant saltation on Mars, *Proc. Natl. Acad. Sci. U.S.A.*, *105*, 6222–6226, doi:10.1073/pnas.0800202105.
- Asphaug, E. (2007), The shifting sands of asteroids, *Science*, *316*, 993–994, doi:10.1126/science.1141971.
- Bi, D., J. Zhang, B. Chakraborty, and R. P. Behringer (2011), Jamming by shear, *Nature*, *480*, 355–358, doi:10.1038/nature10667.
- Boudet, J. F., Y. Amarouchene, and H. Kellay (2006), Dynamics of impact cratering in shallow sand layers, *Phys. Rev. Lett.*, *96*, 158001–4, doi:10.1103/PhysRevLett.96.158001.
- Brzinski, T. A., III, and D. J. Durian (2010), Characterization of the drag force in an air-moderated granular bed, *Soft Matter*, *6*, 3038–3043, doi:10.1039/B926180J.
- Brzinski, T. A., III, P. Mayor, and D. J. Durian (2013), Depth-dependent resistance of granular media to vertical penetration, *Phys. Rev. Lett.*, *111*, 168002, doi:10.1103/PhysRevLett.111.168002.
- Chen, L., P. B. Umbanhowar, H. Komsuoglu, D. E. Koditschek, and D. I. Goldman (2009), Sensitive dependence of the motion of a legged robot on granular media, *Proc. Natl. Acad. Sci. U.S.A.*, *106*, 3029–3034, doi:10.1073/pnas.0809095106.
- Constantino, D. J., J. Bartell, K. Scheidler, and P. Schiffer (2011), Low-velocity granular drag in reduced gravity, *Phys. Rev. E*, *83*, 011305–4, doi:10.1103/PhysRevE.83.011305.
- de Vet, S. J., and J. R. de Bruyn (2007), Shape of impact craters in granular media, *Phys. Rev. E*, *76*, 041306–4, doi:10.1103/PhysRevE.76.041306.
- Dorbolo, S., F. Ludewig, and N. Vandewalle (2013), Bouncing trimer: A random self-propelled particle, chaos and periodical motions, *Granular Matter*, *15*, 033016–033038, doi:10.1088/1367-2630/15/3/033016.
- Elvis, M. (2012), Let's mine asteroids—For science and profit, *Nature*, *485*, 549, doi:10.1038/485549a.
- Goldman, D. I., and P. Umbanhowar (2008), Scaling and dynamics of sphere and disk impact into granular media, *Phys. Rev. E*, *77*, 021308–14, doi:10.1103/PhysRevE.77.021308.
- Katsuragi, H., and D. J. Durian (2007), Unified force law for granular impact cratering, *Nat. Phys.*, *3*, 420–423, doi:10.1038/nphys583.
- Katsuragi, H. (2012), Nonlinear wall pressure of a plunged granular column, *Phys. Rev. E*, *85*, 021301–5, doi:10.1103/PhysRevE.85.021301.
- Kondic, L., X. Fang, W. Losert, C. S. O'Hern, and R. P. Behringer (2012), Microstructure evolution during impact on granular matter, *Phys. Rev. E*, *85*, 011305–17, doi:10.1103/PhysRevE.85.011305.
- Miyamoto, H., et al. (2007), Regolith migration and sorting on asteroid Itokawa, *Science*, *316*, 1011–1014, doi:10.1126/science.1134390.
- Pacheco-Vázquez, F., G. A. Caballero-Robledo, J. M. Solano-Altamirano, E. Altshuler, A. J. Batista-Leyva, and J. C. Ruiz-Suárez (2011), Infinite penetration of a projectile into a granular medium, *Phys. Rev. Lett.*, *106*, 218001–4, doi:10.1103/PhysRevLett.106.218001.
- Ruiz-Suárez, J. C. (2013), Penetration of projectiles into granular targets, *Rep. Prog. Phys.*, *76*, 1–23, doi:10.1088/0034-4885/76/6/066601.
- Shinbrot, T., N.-H. Duong, L. Kwan, and M. M. Alvarez (2004), Dry granular flows can generate surface features resembling those seen in Martian gullies, *Proc. Natl. Acad. Sci. U.S.A.*, *101*, 8542–8546, doi:10.1073/pnas.0308251101.
- Sperl, M. (2006), Experiments on corn pressure in silo cells: Translation and comment on Janssen's paper from 1895, *Granular Matter*, *39*, 59–65, doi:10.1007/s10035-005-0224-z.
- Thomas, P. C., and M. S. Robinson (2005), Seismic resurfacing by a single impact on the asteroid 433 Eros, *Nature*, *436*, 366–369, doi:10.1038/nature03855.
- Uehara, J. S., M. A. Ambrosio, R. P. Ojha, and D. J. Durian (2003), Low-speed impact craters in loose granular media, *Phys. Rev. Lett.*, *90*, 194301–4, doi:10.1103/PhysRevLett.90.194301.
- Walsh, A. M., K. E. Holloway, P. Haddas, and J. R. de Bruyn (2003), Morphology and scaling of impact craters in granular media, *Phys. Rev. Lett.*, *91*, 104301–4, doi:10.1103/PhysRevLett.91.104301.